Department of Chemistry
University of Eastern Finland

102/2010

Merja Niemi

A Molecular Basis for Antibody Specificity – Crystal Structures of IgE-Allergen and IgG-Hapten Complexes

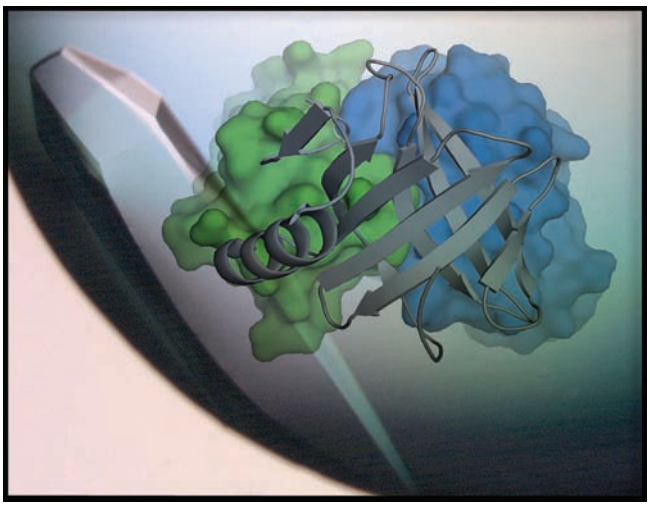

A Molecular Basis for Antibody Specificity - Crystal Structures of IgE-Allergen and IgG-Hapten Complexes

Merja Niemi

Department of Chemistry
University of Eastern Finland
Finland

Joensuu 2010

Merja Niemi
Department of Chemistry, University of Eastern Finland
P.O. Box 111, 80101 Joensuu, Finland

Supervisor
Prof. Juha Rouvinen, University of Eastern Finland

Referees
Prof. Markku Kulomaa, University of Tampere
Docent Anastassios Papageorgiou, University of Turku

Opponent
Prof. Jari Ylänne, University of Jyväskylä

To be presented with the permission of the Faculty of Science and Forestry of the University of Eastern Finland for public criticism in Auditorium F100, Yliopistokatu 7, Joensuu, on May 7th, 2010 at 12 o´clock noon.

ISBN 978-952-61-0124-8
ISBN 978-952-61-0125-5 (PDF)

Joensuun yliopistopaino
Joensuu 2010

ABSTRACT

Antibodies are central proteins of the humoral immune response of vertebrate species. The function of antibodies is based on their capability to specifically recognize the pathogenic antigens. The high diversity and specificity of antibodies has been widely applied to diagnostic, therapeutic, and research applications. In this study, the molecular basis for the function of an allergen binding IgE Fab fragment and two hapten (small molecule) binding IgG Fab fragments was examined by determining crystal structures of the antibodies in complex with their target antigens.

The crystal structure of a recombinant IgE Fab fragment in complex with a bovine beta-lactoglobulin (BLG) allergen was determined at 2.8 Å resolution. BLG, from the lipocalin protein family, is one of the major allergens of cow´s milk and causes food allergy, especially among infants and young children. The solved structure revealed that two IgE molecules were bound to a dimeric allergen. The IgE binding site is located on the planar surface of the BLG allergen and is mainly composed of β-strands. Therefore, the IgE epitope of BLG differs substantially from the common IgG epitopes. This complex structure provided the first insight into IgE antibody-allergen interactions at the molecular level. The findings are expected to be useful in the development of novel approaches to the treatment of allergy.

Steroid hormones are one class of important analytes for which antibodies have been developed during recent years. In this study, the crystal structure of the anti-testosterone Fab fragment 5F2 from a naïve human antibody library was solved at 1.5 Å resolution. The crystal was pseudomerohedrally twinned, which complicated the structure determination. In the solved structure, the testosterone was buried in a hydrophobic binding pocket and the heavy chain of the antibody was mainly interacting with the hapten molecule. The testosterone binding site of the 5F2 Fab with a high abundance of aromatic amino acid residues showed clear similarity with steroid binding antibodies that have been isolated from non-human sources. The solved structure is expected to facilitate the design of specific modifications that could enhance the binding properties of the antibody.

Preparations of the cannabis plant, such as hashish and marijuana, are widely used as illicit drugs in the world. The main psychoactive compound of the cannabis plant is tetrahydrocannabinol (Δ^9-THC). The T3 Fab fragment, generated for the detection of THC in biological samples, was crystallized in the absence and the presence of THC and the crystal structures were solved at 1.9 Å and 2.0 Å resolution, respectively. The T3 Fab binds THC into a narrow pocket between the variable domains of the antibody. In contrast to the 5F2 Fab fragment, the T3 Fab binds the hydrophobic molecule mainly through aliphatic amino acid residues. The solved structure is the first three-dimensional structure of a protein complexed with a psychoactive cannabinoid.

LIST OF ORIGINAL PUBLICATIONS

This dissertation is a summary of the following original publications I-V.

I Niemi M., Jänis J., Jylhä S., Kallio J. M., Hakulinen N., Laukkanen M.-L., Takkinen K. and Rouvinen J. Characterization and Crystallization of a Recombinant IgE Fab Fragment in Complex with the Bovine β-Lactoglobulin Allergen. *Acta Cryst*. F64 **2008**, 25-28.

II Niemi M., Jylhä S., Laukkanen M.-L., Söderlund H., Mäkinen-Kiljunen S., Kallio J. M., Hakulinen N., Haahtela T., Takkinen K. and Rouvinen J. Molecular Interactions between a Recombinant IgE Antibody and the β-Lactoglobulin Allergen. *Structure* **2007**, 15, 1413-1421.

III Kallio J. M., Hakulinen N., Kallio J. P., Niemi M. H., Kärkkäinen S. and Rouvinen J. The Contribution of Polystyrene Nanospheres towards the Crystallization of Proteins. *PLoS ONE* **2009**, 4, e4198.

IV Niemi M. H., Takkinen K., Amundsen L. K., Söderlund H., Rouvinen J. and Höyhtyä M. The Testosterone Binding Mechanism of an Antibody Derived from a Naïve Human scFv Library. *J. Mol. Recognit*., in press.

V Niemi M. H., Turunen L., Pulli T., Nevanen T. K., Höyhtyä M., Söderlund H., Rouvinen J. and Takkinen K. A Structural Insight into the Molecular Recognition of a (-)-Δ^9–Tetrahydrocannabinol and the Development of a Sensitive One-Step, Homogeneous Immunocomplex Based Assay for its Detection. Submitted for publication.

CONTENTS

ABBREVIATIONS

BLG	bovine beta-lactoglobulin
CDR	complementarity determining region
ESI-FTICR	electrospray ionization Fourier transform ion cyclotron resonance
ESRF	European Synchrotron Radiation Facility
Fab	antigen binding fragment of an antibody
Fab 5F2	testosterone binding IgG Fab fragment
Fab D1	beta-lactoglobulin binding IgE Fab fragment
Fab T3	tetrahydrocannabinol binding IgG Fab fragment
Fc	crystallizable (constant) fragment of an antibody
IgE	immunoglobulin E
IgG	immunoglobulin G
K_d	dissociation constant (mol/L)
kDa	kilodalton = 10^3 g/mol
NCS	non-crystallographic symmetry
PDB	Protein Data Bank
PEG	polyethylene glycol
rmsd	root-mean-square deviation
scFv	single-chain variable fragment
SDS-PAGE	sodium dodecyl sulfate polyacrylamide gel electrophoresis
TES	testosterone
THC	Δ^9-tetrahydrocannabinol
Å	ångström = 1×10^{-10} m

1 INTRODUCTION

The immune system of vertebrates has evolved to protect the host from pathogens, such as bacteria and viruses. Immunity can be divided into innate and adaptive immunity. The innate immunity, which provides the first line defence against infections, is composed of elements that are the same in all members of a species. Unlike the innate immunity, the adaptive immunity is highly specific, resulting from a contact with a foreign substance (antigen). Lymphocytes are the type of white blood cells that have a central role in the adaptive immunity. T lymphocytes, or T cells, are involved in the cell-mediated immunity, whereas the humoral immunity is mediated by B lymphocytes (B cells). The principal function of B cells is to produce soluble glycoproteins, known as antibodies. Antibodies are capable of specifically binding to the antigen molecules, thus facilitating their elimination by other components of the immune system.

Two scientists, G.M. Edelman and R.R. Porter, shared the Nobel prize for Medicine 1972, awarded for their discoveries concerning the chemical structure of antibodies. A year later, the three-dimensional structures of two proteins produced by myeloma tumor, the immunoglobulin light chain dimer[1] (Bence-Jones protein) and the Fab fragment of a human immunoglobulin,[2] were characterized by X-ray crystallography. Within the following decades, the structures of hundreds of different antibodies or fragments of antibodies, which recognize a wide variety of antigens from small molecules to large proteins, have been determined experimentally. Although the basic structure of all antibodies is highly similar, each antibody has a unique binding specificity and affinity to the target antigen. Specific recognition originates at the molecular level and is achieved through non-covalent interactions between an antibody and an antigen. The structural characterization of antibody-antigen complexes is essential for understanding the recognition mechanism of an antibody. The knowledge of an antibody structure and its function is also a remarkable benefit for protein engineering.

1.1 THE GENERAL STRUCTURE OF ANTIBODIES

The basic structure of an immunoglobulin molecule consists of two light chains and two heavy chains connected together by disulfide bonds. The light and heavy chains of an antibody are folded into domains, each containing about 110 amino acid residues. The antiparallel β-strands of a domain arrange in two layers of β-sheets, which pack closely against each other. This characteristic beta-sandwich structure has also been found in other proteins and is commonly known as the immunoglobulin fold (Figure 1).

The amino acid sequence variation in antibodies is located in the amino-terminal variable domains of both the heavy chains and the light chains. Meanwhile, the

diversity of the remaining constant domains is more limited among the antibodies that belong to the same class.

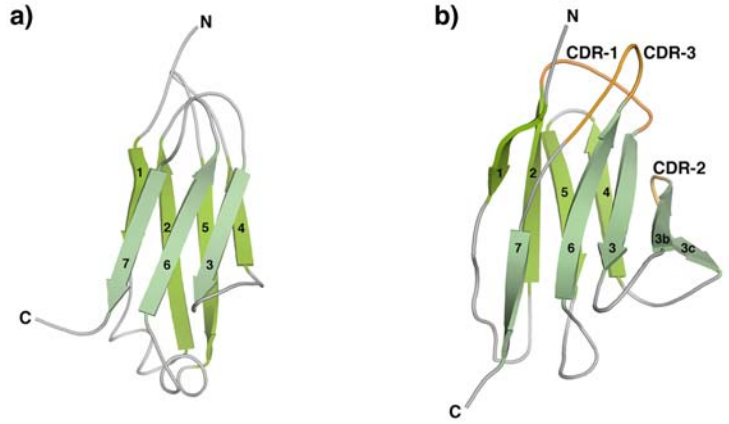

Figure 1. The immunoglobulin fold. The constant domain (a) consists of seven antiparallel β-strands. The variable domain (b) contains two additional strands, 3b and 3c. CDR-loops that connect β-strands 2-3, 3b-3c, and 6-7 are shown in orange.

The most diverse regions of a variable domain occur in three loops that connect the adjacent β-strands. An antibody binds an antigen mainly through these complementarity determining regions (CDRs), which are clustered together in the structure of a folded antibody (Figure 1b). The enormous diversity and binding specificity of antibodies is mainly reached by varying the amino acid composition and the length of the CDR-loops.

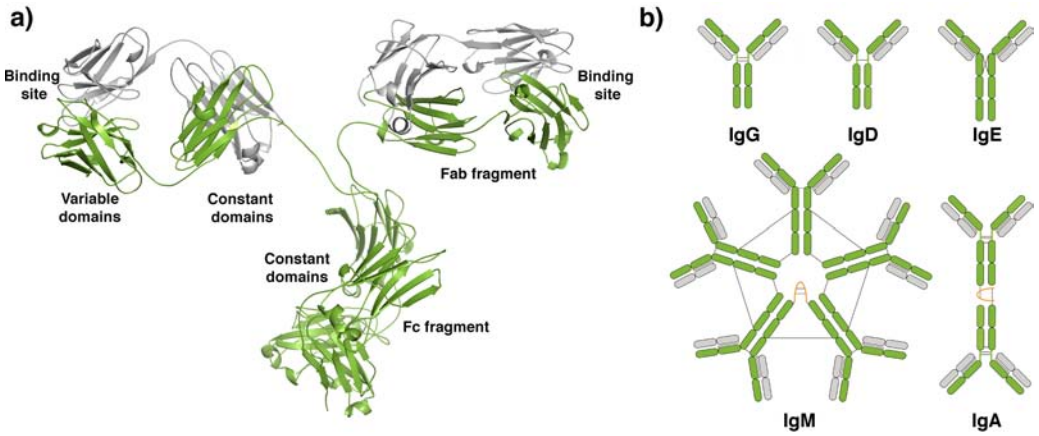

Figure 2. a) The basic structure of an immunoglobulin G (IgG, PDB code 1IGT[3]). The molecular weight of an IgG is around 150 kDa and the molecule consists of two Fab fragments (Mw ~50 kDa) and one Fc fragment. The light chains of the antibody are shown in gray and the heavy chains are in green. b) Schematic structures of antibodies of five main classes. Disulfide bonds are shown as black thin lines.

The controlled cleavage by a proteolytic enzyme papain degrades an intact immunoglobulin into fragments. The antigen binding fragment (Fab) contains the entire light chain (VL, CL) combined with the variable VH and constant CH1 domains of the heavy chain, whereas the Fc fragment involves the rest of the constant domains of the heavy chain. While the specificity of an antibody is primarily centered in the CDR loops of the variable domains, the constant domains of the heavy chain mediate the effector functions. Antibodies are divided into classes based on the properties of the heavy chain (Figure 2b). Five antibody classes (IgA, IgD, IgE, IgG and IgM) have different heavy chain isotypes, which define the biological activity of the antibody. One of the two light chain types (kappa or lambda) can associate with each of these heavy chain isotypes. No functional differences have been observed in the light chain classes.

1.2 IGE-MEDIATED (TYPE 1) HYPERSENSITIVITY

Allergies are caused by an inappropriate immune response against non-pathogenic substances, known as allergens. In the developed countries, asthma and other allergic disorders such as hay fever, eczema and even life-threatening anaphylaxis, have become a serious problem for public health.[4] The type 1 allergy initiates the production of allergen-specific class E (IgE) antibodies on B cells. IgE antibodies secreted by B cells are capable of sensitizing blood basophiles and tissue mast cells by binding to high-affinity FcεRI receptors located on their surface. The simultaneous binding of two membrane-bound IgE antibodies to an allergen molecule induces the cross-linking of receptors, which triggers the cells to release histamine and other biological mediators, thus causing an allergic inflammation (Figure 3).

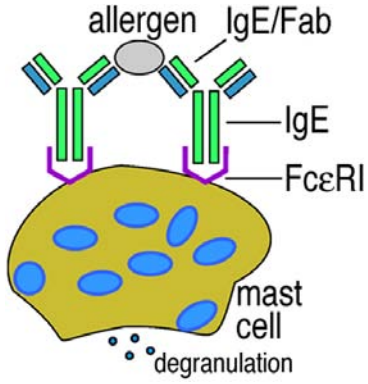

Figure 3. Degranulation of a mast cell.

Allergens are almost exclusively proteins that are present in the common substances of daily life, such as food products, tree and grass pollens and animal dander. The

biochemical and the structural characterization of a large number of allergenic proteins have not revealed any common feature that could explain their capacity to induce IgE production.[5] However, evidence that the structural properties of proteins may also have some effect on allergies has been obtained in recent years: the structural classification of allergens has revealed that only a limited number of protein families contain allergens.[6,7] In addition, certain allergen-specific IgG antibodies bind allergens with a lower affinity than corresponding IgE antibodies[8] and some allergens are weak immunogens that do not stimulate IgG production very well.[9,10] These results suggest that allergens may have some unique structural features, which are not easily available for IgG antibodies but are, in contrast, recognized by IgE antibodies.

An allergen-specific IgE binds to an immunologically active region of an allergen, i.e. a B cell epitope. Since the allergic reactions arise from the interactions between the IgE and allergen, the identification of B cell epitopes has been the major interest in allergy research. Although B cell epitopes have been sought by several methods (e.g. epitope mapping and site-directed mutagenesis), the rational method to determine a complete B cell epitope is to solve the crystal structure of an allergen-specific IgE in complex with the allergen.[11] However, the low abundance of IgE in the serum of even the most severely allergic patients and the failure to produce monoclonal IgE antibodies by conventional hybridoma technology have been the major obstacles for accessing IgE for structural studies.

1.3 ANTIBODIES IN DIAGNOSTICS AND THERAPY

The specific recognition of antibodies has been widely utilized in immunodiagnostic and therapeutic applications. A number of important analytes, including the steroid hormones and drugs, are small organic molecules that contain only a few functional groups and exist at a low concentration in biological samples. The selective and specific recognition of the particular analyte may be achieved by using high-affinity antibodies. The production of antibodies specific for small molecules (haptens) requires that a hapten is conjugated to a carrier protein, because small molecules cannot induce the immune response by themselves. Advances in biotechnology, especially the availability of large antibody phage libraries, have allowed the generation of antibodies against an almost unlimited variety of molecules.[12-15] Human phage display libraries have also enabled the selection of human antibodies for immunotherapy.[15-17]

Immunoassays that are based on specific antibody-antigen interactions are commonly used in diagnostics. The sensitivity of traditional immunoassays has been further improved by developing non-competitive immunoassays, where two antibodies bind the different epitopes of the target analyte. Non-competitive immunoassays have also been generated for the detection of several low molecular weight analytes.[18-21] In these novel assays, the limitation caused by the size of the analyte is overcome by the use of anti-immunocomplex (anti-IC) antibodies that specifically recognize the complex

formed between the primary antibody and the analyte. The binding properties of antibodies can be modified in order to improve the affinity and the specificity towards the analyte or to decrease the cross-reactivity with closely related molecules, thus improving the accuracy and the reliability of immunoassays.

The development of therapeutic antibodies is a continuously growing area in the pharmaceutical industry.[22] So far, therapeutic monoclonal antibodies are available for the treatment of several diseases, e.g. virus infections and cancer. In human immunotherapy, the use of murine antibodies can cause side effects and evoke an immune response, which reduces the efficiency of the therapy. Therefore, the humanized antibodies and the fully human antibodies isolated from gene libraries are of particular interest for the development of new therapeutic applications.

2 AIMS OF THE STUDY

The general purpose of this study was to determine the crystal structures of three different antibody-antigen immunocomplexes by X-ray crystallography, in order to understand the relationship between the structure and the function of the antibodies. The specific aims were as follows:

1. To crystallize and solve the structure of a recombinant IgE Fab fragment in complex with the bovine beta-lactoglobulin, one of the major allergens of cow´s milk. Before this study, the structures of IgE antibody-allergen complexes had not been determined. The complex structure was expected to yield new information about the IgE-allergen interactions that could extend the knowledge of the molecular mechanism of allergies and might also be useful in the development of novel applications for the treatment of allergic disorders.

2. To crystallize and determine the three-dimensional structure of an anti-testosterone Fab fragment 5F2 in complex with its specific hapten. 5F2 Fab was isolated from a naïve human phage display library, in contrast to previously characterized mouse anti-testosterone Fab fragments. By solving the structure, it would be possible to compare the mouse and human antibodies that bind an identical molecule. Knowledge of 5F2 Fab-testosterone interactions also enables the modification of selected amino acids that could improve the binding specificity and affinity of the antibody.

3. To crystallize and determine the structure of an anti-tetrahydrocannabinol Fab fragment T3 in free form and in complex with Δ^9-tetrahydrocannabinol (THC), the major psychoactive compound of *Cannabis sativa*. The three-dimensional structure of the T3 Fab in complex with THC would provide the first insight into the molecular interactions between a protein and the Δ^9-tetrahydrocannabinol. Because the T3 Fab was generated for the detection of THC in biological samples, the information on T3 Fab-THC interactions could also be useful for designing specific mutations, so that the antibody fits the target application better.

3 MATERIALS AND METHODS

All materials and methods of the study are described in detail in the original publications I-V. A brief summary is presented below.

Fab fragments were isolated, produced and purified at the VTT Technical Research Centre of Finland. The VL and VH regions of a D1 antibody were isolated from IgE ScFv phage display library, constructed from lymphocytes of a milk allergic patient. The isolated IgE scFv fragment was converted to a Fab fragment by cloning the CH1 and CL regions from a human IgG1 heavy chain and kappa light chain to variable domains of D1 antibody. The genes encoding the D1 Fab fragment were cloned into the bacterial expression vector (pKKtac)[23] and the Fab fragment was produced by high-cell density fermentation of *E. coli* strain RV308. The expressed Fab fragment with the C-terminal hexahistidine tag was purified by immobilized metal ion affinity chromatography. The purity and homogeneity of the protein solution was checked by non-reducing SDS-PAGE and ESI-FTICR mass spectrometry. D1 Fab binds native BLG with nanomolar affinity (K_d 1.3×10^{-9} M) and partially inhibits serum IgE to bind BLG.[24] BLG (Mw ~18.3 kDa) from bovine milk is a commercially available protein ordered from Sigma Aldrich.

The small molecule binding Fab fragments 5F2 and T3 were produced and purified by a procedure similar to that described for the D1 Fab fragment. The anti-testosterone Fab 5F2 was isolated from a naïve human phage display library. 5F2 Fab has the IgG heavy chain combined with the type lambda light chain. The binding affinity of 5F2 Fab to testosterone is ~900 nM, determined by competitive ELISA. The anti-tetrahydrocannabinol Fab T3 was isolated from a phage display library, constructed from mice immunized with a THC-BSA conjugate. T3 is a Fab fragment of IgG antibody with the kappa light chain. The binding affinity of T3 Fab to THC is ~500 nM. Both testosterone and Δ^9-THC were purchased from Sigma Aldrich. THC was used in crystallization with the permission of the Finnish Medicines Agency.

All Fab fragments were crystallized by the hanging-drop vapor-diffusion method at room temperature using PEG3350 as a precipitant. X-ray diffraction data sets were collected at cryo-temperature (100 K) using synchrotron radiation at the ESRF, Grenoble. The diffraction images were processed by using XDS and scaled and merged with XSCALE.[25] Antibody structures were solved by the molecular replacement method, using previously determined Fab structures as search models. The principal selection criteria for the search models were their high sequence identity with the target protein. The rotation and the translation functions were determined separately for the variable domains and the constant domains of an antibody. The protein models were built up by several refinement cycles and manual fitting with the program O.[26] The topology files for hapten molecules were created with PRODGR.[27] The solvent accessible surfaces were calculated with AreaImol from the CCP4 program package[28] and the program NCONT (CCP4) was used to search the contacts between the antibody and the antigen. The elbow angles of the Fab fragments were determined with

RBOW.[29] The stereochemical quality of the antibody structures was confirmed with the ADIT[30] validation server.

4 RESULTS AND DISCUSSION

4.1 PROTEIN CRYSTALLOGRAPHY

4.1.1 CRYSTALLIZATION[I, III, IV, V]

The conditions that favor the nucleation process are not generally optimal for the controlled growth of protein crystals. Therefore, the crystals obtained from the initial crystallization experiment are not usually of sufficient size and quality for X-ray analysis. The careful optimization of the crystallization conditions or the use of crystallization additives may be crucial to the growth of high-quality crystals. The spontaneous nucleation step can also be bypassed by introducing nuclei into a crystallization drop at a lower level of supersaturation. In the commonly used streak-seeding method, the transferred nuclei are obtained from previously grown protein crystals. If pre-existing crystals are not available as a source of nuclei, the introduction of heterogeneous material into a crystallization droplet may promote the nucleation of a protein. Besides other optimization methods, a new class of heterogeneous nucleant, polystyrene nanospheres, was tested in the crystallization of the 5F2 and T3 Fab fragments. Polystyrene nanospheres with different particle diameters are commercially available calibration standards for electron and atomic force microscopy.

The D1 Fab fragment precipitated when the concentration of the protein solution was increased. Therefore, a D1 Fab concentration of 1.4 mg/ml was used in the crystallization experiments. The lyophilized BLG was dissolved into pure water to a concentration of 2 mg/ml. D1 Fab-BLG complex crystals were obtained using a 14% (w/v) PEG3350, 0.1 M BTP solution at pH 5.0. Initial crystals grew as clusters of thin needles from which single crystals were not possible to separate. The addition of a *n*-dodecyl-β-D-maltoside detergent solution to crystallization droplets proved to be essential for the growth of three-dimensional crystals. Microcrystal with approximate dimensions of 0.07 × 0.05 × 0.05 mm appeared in the crystallization droplets within a week (Figure 4a).

Anti-testosterone Fab 5F2 was co-crystallized with the hapten using a 12% (w/v) PEG3350, 0.1 M sodium citrate at pH 4.7 as a precipitant solution. The 5F2 Fab concentration was ~8 mg/ml and an 8-fold excess of testosterone was used in crystallization. Single 5F2 Fab crystals suitable for X-ray analysis were obtained by combining the streak-seeding method with the polystyrene nanospheres. Crystal dimensions were approximately 0.2 × 0.1 × 0.1 mm (Figure 4b). Attempts to crystallize 5F2 Fab without the testosterone were unsuccessful.

Anti-tetrahydrocannabinol Fab fragment T3 was crystallized both in the absence and the presence of THC. The concentration of T3 Fab in crystallization experiments was ~ 18 mg/ml. The optimal precipitant solution for the uncomplexed T3 Fab was found to be a 14 % (w/v) PEG3350, 0.1 M sodium citrate at pH 5.2. Crystals grew up to dimensions of 0.6 × 0.3 × 0.2 mm within a week (Figure 4c). In co-crystallization experiments, a 10-fold excess of hapten was used. The T3 Fab-THC complex was crystallized with a 12% (w/v) PEG3350, 0.1 M sodium HEPES solution at pH 7.5. As the initial complex crystals were spherical in shape, a nanosphere solution and the streak-seeding method were used to improve the quality of the crystals. Single crystals with dimensions of 0.1 × 0.1 × 0.05 mm were obtained within 2-3 days after the seeding (Figure 4d).

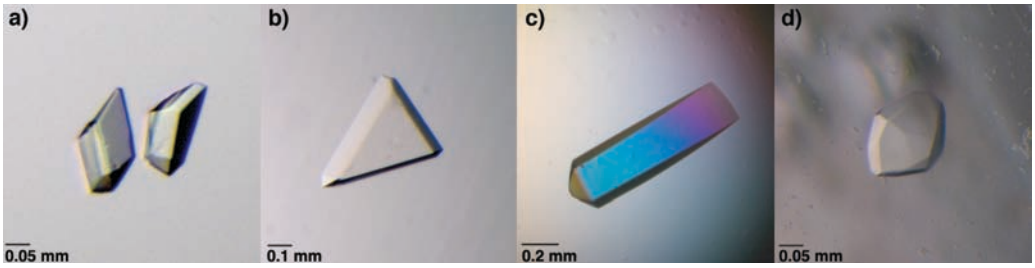

Figure 4. Protein crystals: a) D1/BLG b) 5F2/TES c) T3 d) T3/THC. The black bars indicate the estimated crystal sizes.

4.1.2 DATA COLLECTION AND PROCESSING[I, IV, V]

Summary of the data collection and processing statistics are presented in Table 1.

Table 1. Data collection and processing statistics. Values in parentheses are for the highest resolution shell.

	D1/BLG	5F2/TES	T3	T3/THC
Beamline	ID29	ID29	ID14-4	ID14-4
Space group	$P2_12_12_1$	P1	$P4_32_12$	$P4_32_12$
Unit cell parameters				
a, b, c (Å)	67.0, 100.6, 168.1	66.8, 67.1, 67.1	121.4, 121.4, 73.5	122.8, 122.8, 73.3
α, β, γ (°)	a = b = c = 90	81.3, 69.3, 69.3	a = b = c = 90	a = b = c = 90
Resolution (Å)	2.8 (2.9-2.8)	1.5 (1.6 -1.5)	1.9 (2.0-1.9)	2.0 (2.1-2.0)
No. of reflections	207474	299821	390342	272030
Unique reflections	28674	151891	43799	38070
R_{obs} (%)	15.9 (55.2)	3.3 (32.1)	5.4 (38.6)	3.9 (44.5)
R_{meas} (%)	17.2 (59.4)	4.7 (45.3)	5.7 (41.6)	4.2 (47.9)
Average I/σ	13.1 (3.5)	14.0 (2.5)	22.7 (5.1)	28.4 (4.5)
Completeness (%)	99.8 (100)	93.1 (91.0)	100 (100)	99.2 (99.9)

4.1.3 STRUCTURE DETERMINATION AND REFINEMENT[II, IV, V]

The D1 Fab-BLG complex structure was solved using the Fab fragment of the human IgG antibody specific for the transmembrane protein gp41 of the HIV-virus[31] (PBD code 1DFB) and a BLG monomer[32] (1B8E) as search models. Molecular replacement was carried out with MolRep[33] and the complex structure was refined with the program CNS.[34] Because of the low number of unique reflections, NCS restraints were used in refinement.

The search model for the 5F2 Fab was the VLA-1 integrin 1 domain binding Fab fragment of a humanized AQC2 antibody[35] (PDB 1MHP). The structure refinement was carried out with PHENIX.[36] Coordinates for the testosterone were obtained from a previously determined Fab-testosterone structure.[37]

The structure of the THC binding Fab fragment T3 was solved using the Fab fragment of a catalytic antibody 6D9[38] (2DQT) as a search model. The long CDR-loops of the search model were deleted before the molecular replacement was carried out. The molecular replacement was performed with Phaser[39] and the structure was refined with PHENIX. The initial coordinates for hapten were obtained from a modelled THC structure. The refinement statistics are presented in Table 2.

Table 2. Refinement statistics and validation.

	D1/BLG	5F2/TES	T3	T3/THC
R_{work} (%)	24.6	17.9	21.4	21.4
R_{free} (%)	29.1	20.8	24.3	26.1
No. of atoms	9136	7532	3547	3566
Protein	9066	6571	3287	3302
Hapten	-	42	-	24
Additive	70	-	-	-
Water	-	919	260	240
Average B ($Å^2$)	27.4	20.1	34.2	39.2
Rms deviations				
Bond lengths (Å)	0.009	0.013	0.013	0.012
Bond angles (°)	1.2	1.7	1.5	1.6
PDB code	2R56	3KDM	3LS5	3LS4

4.1.4 NANOSPHERES IN THE CRYSTALLIZATION OF FAB FRAGMENTS[III]

The initial 5F2 Fab fragment crystals grew in clusters. Although single crystals were obtained by the streak-seeding method, the crystallization droplets required a long equilibration time (2-3 weeks) before the seeding. When nanospheres (50 nm in diameter, 1:1 dilution to water) were added to droplets prior to seeding, substantially shorter equilibration times could be used: single crystals appeared in droplets, which were allowed to equilibrate for only 24 hours. The growing of diffraction-quality crystals in the presence of nanospheres was still dependent on the use of seeding. Otherwise, the crystals grew in clusters in nanosphere droplets. The combination of the polystyrene nanospheres with the streak-seeding method also proved to be an efficient technique for producing T3 Fab-THC crystals for structure determination. The use of nanospheres and seeding improved the quality of complex crystals. By contrast, in similar conditions, the traditional streak-seeding method yielded crystals that were of poor quality, visually. The effect of nanospheres on the crystallization of complexed T3 Fab without seeding was not examined.

Although polystyrene nanospheres were observed improving the quality of the protein crystals and affecting the equilibration time of crystallization droplets, the mechanism by which nanospheres function is not clear. It is possible that nanospheres act as a heterogeneous nucleant, providing a regular surface onto which protein molecules can assemble. The alternative explanation is that nanospheres take up space in solution, in which case the protein molecules can cluster closer together and form crystal nuclei.

4.1.5 TWINNING IN A 5F2 FAB CRYSTAL[IV]

Pseudomerohedral twinning may occur in a protein crystal as a consequence of unusual unit-cell geometry. In a pseudomerohedrally twinned crystal, the metric symmetry of the lattice is higher than the Laue symmetry of the crystal.[40,41] A triclinic crystal can be pseudomerohedrally twinned if the two axes and two angles of the cell appear to be almost equal. This kind of twinning where a triclinic crystal mimics a monoclinic one has been previously noticed in an RNA fragment crystal.[42] The structure of 5F2 Fab was initially solved in space group C2. Twinning was detected when the electron density maps revealed two alternative positions for the polypeptide chain near the crystallographic twofold axis (Figure 5a). The data were indexed in space group P1 and the twin law *-h, -l, -k* was introduced into the structure refinement. The twin refinement decreased both the crystallographic R-factors and improved the quality of the electron density maps (Figure 5b).

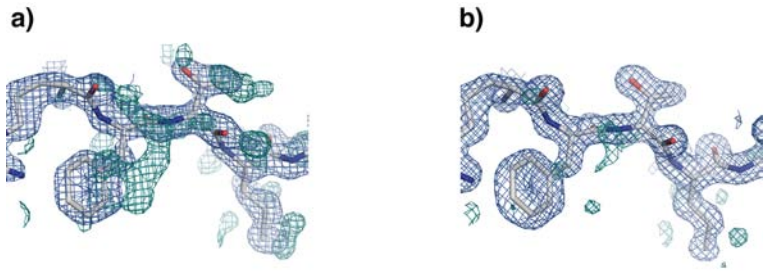

Figure 5. A portion of electron density maps. a) Electron density near the crystallographic twofold axis when the structure was refined in space group C2. b) The same area after the twin refinement in space group P1. The $2F_o$-F_c map (blue) is contoured at 1.5 σ and the F_o-F_c map (green) at 2.5 σ.

4.2 THE IGE FAB-ALLERGEN COMPLEX D1/BLG[II]

The three-dimensional structure of the IgE Fab-allergen complex D1/BLG was solved at 2.8 Å resolution. The asymmetric unit contained two D1 Fab fragments bound to a dimeric allergen (Figure 6), representing the entire immunocomplex. The structure of the allergen in complex corresponds to a previously determined BLG structure.[43] BLG monomers are folded into a native β-barrel structure, where eight antiparallel β-strands form the core of the protein. The structure is stabilized with two intramolecular disulfide bonds formed between the cysteine residues of the BLG. BLG is known to bind a number of small molecules, such as fatty acids[44,45] and retinol,[46] inside the hydrophobic binding cavity. The electron density found in the binding site of both BLG monomers was interpreted as a detergent molecule, used to improve the quality of the complex crystals. The hydrophilic maltoside moiety of the detergent is located outside the binding cavity, but is far away from the bound IgE antibody. The location

of a non-crystallographic 2-fold symmetry axis between the BLG monomers was also equal to that observed in a native BLG dimer.[43]

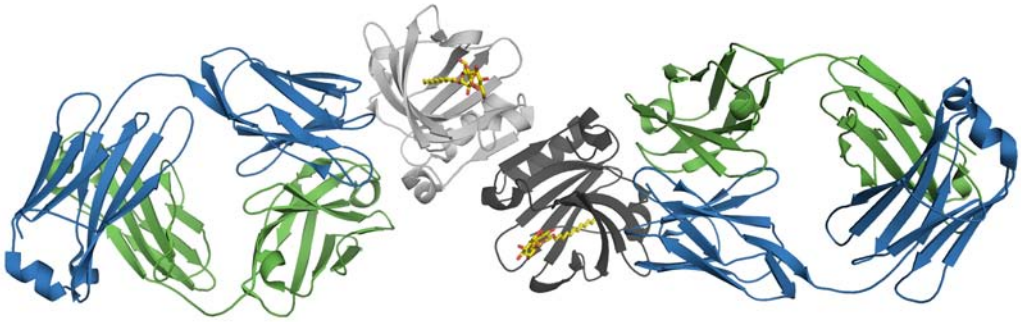

Figure 6. The overall structure of the IgE antibody-allergen immunocomplex. The figure shows how two D1 Fab fragments (light chain in blue, heavy chain in green) bind the dimeric beta-lactoglobulin allergen. Allergen monomers are shown in light and dark gray and the detergent molecules are in yellow.

The variable domains of the D1 Fab fragment follow the typical immunoglobulin fold described for variable domains of common IgG antibodies. All three CDR-loops of the light chain and the CDR-H1 and CDR-H2 loops of the heavy chain belong to known canonical classes of immunoglobulins.[47] The CDR-H3 loop with the bulged conformation in the torso region[48] is a relatively long loop with 17 amino acid residues. The H3-loop is folded towards the other CDR-loops, creating the flat binding site of the antibody. The calculated elbow angles of the D1 antibodies are 141° and 150°, which are common values for Fab fragments containing a kappa light chain.[29] The total interface area of the antibody-allergen complex is large (1825 $Å^2$), but does not substantially deviate from the average interface area (1680 $Å^2$) of protein antigen-antibody complexes.[49]

4.2.1 THE IGE BINDING SITE OF BLG

The D1 Fab recognizes a conformational epitope, which is located on a planar surface of the BLG allergen (Figure 7a). The IgE binding site is similar in both BLG monomers and the epitope area does not extend to the surface of the second monomer or to the dimer interface. The complete IgE epitope of native BLG consists of six short fragments of the polypeptide chain, which are mainly located in the secondary structure elements of the protein (Figure 7b). In the complex structure, 15 amino acid residues of BLG (9 % in total) are in contact with an antibody and 27 amino acid residues (17% in total) are at least partially buried under the bound antibody. The buried area is 890 $Å^2$, which covers 10% of the surface of the BLG monomer. The

major part of the epitope consists of the four adjacent β-strands: segment 1 (Trp19-Tyr20), segment 2 (Val43-Lys47), segment 3 (Leu57-Gln59) and segment 4 (Cys66-Gln68). In addition, the loop between the eighth β-strand of the BLG and the following α-helix (segment 5, Pro126-Glu127) and the short C-terminal helix (segment 6, Thr154-Glu157) form the IgE binding site of BLG.

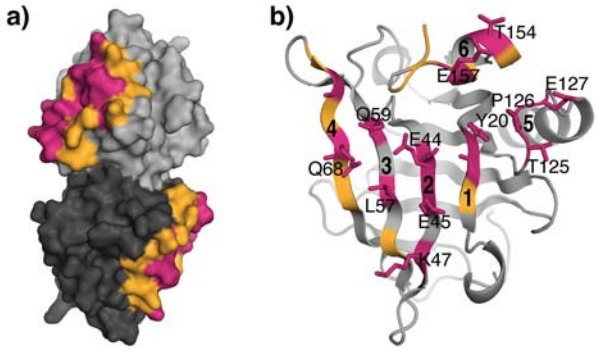

Figure 7. The IgE epitope of the beta-lactoglobulin.[II] a) Location of two monovalent epitopes on the surface of a dimeric allergen. b) The complete IgE epitope of the BLG consists of six short fragments, numbered from 1 to 6. The residues that are in contact with the D1 antibody are colored red and the residues that are buried upon the complex formation are colored in orange.

All six CDR-loops of the D1 Fab participate in allergen binding (Figure 8a). In total, 13 hydrogen bonds and 2 salt bridges are formed between the antibody and the allergen. Only two of the interacting amino acids are aromatic, which is unusual.[49,50] The heavy chain of D1 Fab dominates the interactions between the antibody and allergen, as commonly observed in determined antibody-antigen complexes. The light chain of D1 Fab is responsible for binding three adjacent β-strands of BLG (segments 2, 3 and 4): CDR-L1 (Ser30L, Ser31L and Arg32L) interacts with segments 3 and 4 and CDR-L2 (Tyr49L, Ala50L and Ser52L) interacts with segments 2, 3 and 4. CDR-L3 has a minor role in binding the β-strand region of the BLG. One hydrogen bond is formed between the Tyr91L from CDR-L3 and the Gln68 from segment 4. Besides the named interactions, His92L is within 4.0 Å of Glu66 located before segment 4 and may, thus, raise the contribution of the CDR-L3 to allergen binding.

His31H from CDR-H1 interacts with Pro126 and Glu127 from the loop region of the BLG (segment 5). CDR-H2 takes part in binding the short C-terminal helix (segment 6) through two serine residues, Ser52H and Ser54H. CDR-H3 is located in the middle of the variable domains and has a central role in antigen binding. In complex structure, Arg101H on the tip of the CDR-H3 loop reaches a small cavity formed between the C-terminal helix and β-strands A and B of BLG, interacting with residues from segment 1 and 2. Val102H from CDR-H3 region contributes to allergen binding by recognizing Tyr20 from segment 1 and Pro126 from segment 5.

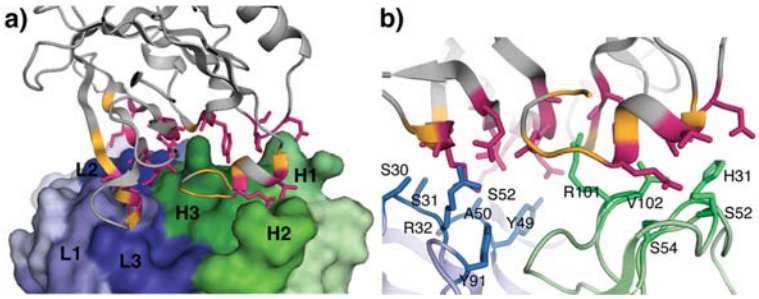

Figure 8. Contacts between the D1 Fab and the BLG.[II] a) Location of the CDR-regions on the surface of the D1 Fab. b) The interacting amino acid residues of the D1 Fab.

4.2.2 THE DIMERIC NATURE OF THE ALLERGEN

Besides an allergen being capable of inducing specific IgE production, it should also contain multiple IgE binding sites for an effective cross-linking of two IgE-FceRI complexes. This requirement means that at least two IgE antibodies with different binding specificities should occur on the surface of basophiles or mast cells and these antibodies should bind an allergen simultaneously. When an allergen is a small protein, the surface area is limited and the requirement of various epitopes is hard to fulfill. The alternative way for an allergen to cross-link the receptors is oligomerization. If an allergen is able to form a dimer or larger oligomers, one epitope in each allergen monomer is sufficient to cause the cross-linking of receptors. This may increase the protein´s capability to operate as an allergen.

The oligomerization state of beta-lactoglobulin is known to be dependent on several parameters, such as pH, temperature and protein concentration.[51,52] In physiological conditions, BLG predominantly exists as a dimer. The minimum distance of receptor-bound IgE molecules linked by a natural allergen has not been reported. Based on the studies conducted on artificial antigens, the distance between the cross-linked IgE molecules has been estimated to be 5-24 nm (50-240 Å).[53,54] The length of the dimeric BLG is around 7 nm, and the distance between the bound D1 Fab molecules in the complex structure is approximately 5 nm. The relative position of the monovalent IgE-epitopes of BLG and the distance between the bound D1/IgE molecules thus enables the cross-linking of FceRI receptors. Although several allergens have been observed to appear as dimers or larger oligomers in nature, including the animal allergens Can f 1 and Can f 2 from dog,[55] Equ c 1[56] from horse and Fel d 1[57] from cat, timothy grass pollen allergens Phl p 1[58] and Phl p 7[59], and food allergens Ara h 1[60,61] and Ara h 2[62] from peanut, the significance of oligomerization for protein allergenicity has been insufficiently examined. However, Schöll *et al*. have recently shown that the dimeric, not the monomeric, form of the birch pollen allergen Bet v 1 was able to cross-link IgE antibodies in mice.[63]

4.2.3 COMPARISON OF IGE AND IGG EPITOPES

The major part of the IgE binding site of BLG is composed of a planar β-sheet region. A comparison with over 80 different antibody-antigen complexes showed that the IgE epitope of BLG is unique among the common IgG epitopes of protein antigens. The typical IgG epitope is located on the protruding or concave surface of an antigen. An analysis of IgG epitopes also revealed that half of the epitopes were formed by loops alone, and the other half contained both loops and secondary structure elements. Recently determined IgG-allergen structures exemplify the common IgG-type binding: in birch pollen allergen Bet v 1[64] the epitope is formed by a β-hairpin; in bee venom hyaluronidase Api m 2,[65] the epitope is a helix-turn-helix motif; and in German cockroach allergen Bla g 2,[66] the epitope is composed of loops. The recently solved structure of the complex between the timothy grass pollen allergen Phl p 2 and human IgE-derived Fab huMab2[67] is in agreement with the hypothesis that IgE antibodies prefer different binding sites than IgG antibodies. In this complex, the IgE epitope of the Phl p 2 is located on the planar four-stranded β-sheet region on the surface of the allergen. Similarly, with D1 antibody, the Phl p 2-specific IgE Fab also binds the allergen with high affinity (K_d 1.1 × 10^{-10} M).

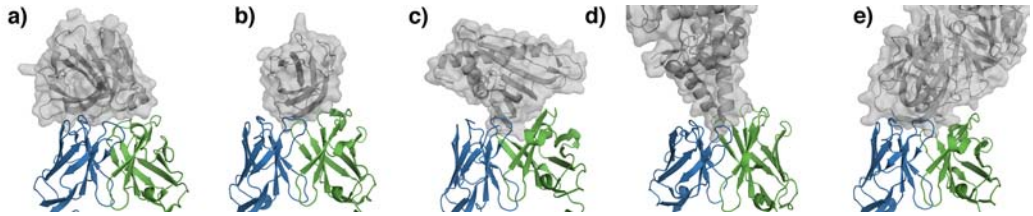

Figure 9. A comparison between IgE and IgG epitopes. a) BLG-IgE/Fab[II] b) Phl p 2-IgE/Fab[67] c) Bet v 1-IgG/Fab[64] d) Api m 2-IgG/Fab[65] e) Bla g 2-IgG/Fab.[66]

4.2.4 SEQUENCE SIMILARITY BETWEEN IGE ANTIBODIES

Both the BLG-specific IgE Fab fragment D1 and the Phl p 2-specific IgE fragment huMab2 were selected from the phage display libraries constructed from lymphocytes of allergic patients. The pairing of the heavy chain and the light chain is not, therefore, necessarily the same as in the complete IgE molecules that naturally occur in patient serum. However, both of these IgE Fab fragments inhibit the serum IgE from binding with the cognate allergen. So far only a few sequences of allergen-specific IgE antibodies have been characterized.[68-71] The heavy chain amino acid sequences of these IgE antibodies vary substantially, whereas some of the light chains share a high sequence homology, especially the CDR-L1 and CDR-L2 loops. The light chain similarity occurs also between D1 Fab and huMab2. Although the light chain of D1 Fab recognizes the β-sheet region on BLG, the light chain of the Phl p 2-specific

antibody is not in contact with the planar β-sheet region of the allergen. Because only two structures of IgE-allergen complexes have been solved by X-ray crystallography,[11,67] the connection between the light chain sequence homology and the nature of the B cell epitope is difficult to evaluate. At least in the D1 antibody, the light chain CDR-loops are responsible for binding the flat β-sheet region on the allergen surface.

4.2.5 SIGNIFICANCE TO ALLERGEN IMMUNOTHERAPY

Allergen-specific immunotherapy has been used for the treatment of allergic diseases for almost a century. The method is based on controlled exposure to a sensitizing allergen that gradually modulates the immune system out of the IgE-mediated response. The mechanisms of immunotherapy are complicated, including several changes in T cell and B cell response and in the expression levels of different antibody classes.[10] The changes involve a strong increase in the serum IgG concentration[72,73] and the enhancement of the blocking activity of IgG antibodies.[74] It has been proposed that the allergen-specific IgG antibodies are able to compete with IgE for allergen binding and inhibit the allergen-induced mast cell and basophils degranulation, and that they may prevent the IgE-facilitated presentation of allergens to T cells.[10,75]

Recombinant allergens have several advantages over the conventionally used crude allergen extracts, which are prepared from natural allergen sources and usually contain a diverse amount of allergenic and non-allergenic proteins.[76] While wild-type recombinant allergens have structural and immunological properties similar to natural allergens, further genetic engineering of allergen molecules has been used to produce modified allergen derivatives.[77] Modified allergens with a reduced IgE binding capacity (i.e. hypoallergens) are considered safer and more efficient molecules for immunotherapy. Allergen derivatives used in immunotherapy should not induce severe IgE-mediated side effects and they have to be well tolerated. Meanwhile, the treatment has to be successful and quickly offer long-term protection with few doses.[78]

The solved immunocomplex structure gave new information about the IgE antibody-allergen interactions. The finding that the IgE antibodies seem to prefer different binding sites of an allergen than IgG antibodies is expected to be valuable in designing novel hypoallergens for allergen-specific immunotherapy. If the three-dimensional structure of an allergen is known, the potential IgE epitopes may be identified on the surface of an allergen and the binding strength of IgE to the allergen could be decreased by modifying the selected amino acid residues.

4.3 THE ANTI-TESTOSTERONE FAB FRAGMENT 5F2[IV]

The space group P1 contained two 5F2 Fab fragments in the asymmetric unit. The high-resolution data of 1.5 Å enabled a clear structure determination. Based on electron density, the N-terminal glutamic acid of the heavy chain was displaced with the cyclic pyroglutamic acid. High flexibility was noticed in the constant domain loop between the residues Ser136H and Gly142H. The loop is frequently disordered in antibody structures.

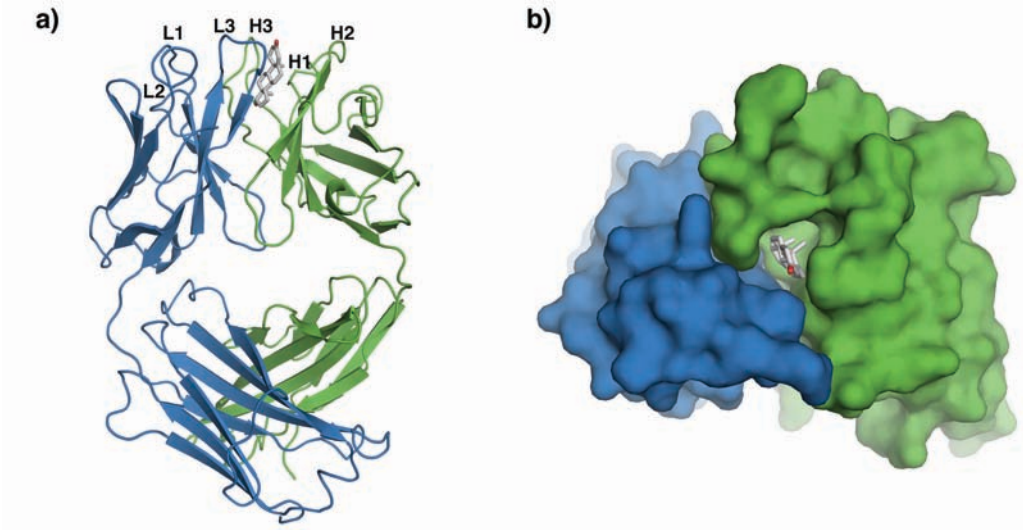

Figure 10. The overall structure of the 5F2 Fab in complex with testosterone. The 5F2 Fab fragment is presented as a cartoon model (a) and a surface model (b). Testosterone is shown as a gray stick model.

The overall shape of an antigen binding site of an antibody tends to correlate with the type of the antigen.[79] Small molecule binding antibodies frequently have long L1 and H2 loops, which create a concave geometry on the surface of the variable domains.[80,81] Although 5F2 Fab has long CDR-L1 (14 residues) and CDR-H2 (17 residues), the loops are folded into conformations that create a flat rather than concave antigen binding site (Figure 10a). The CDR-L1 forms a distorted helix, which is a typical conformation for canonical class 2 loops of a lambda chain. CDR-H2 belongs to class 3 where the apex of the loop is bent toward the surface of the antibody. Whereas the hapten binding antibodies favor short CDR-H3 loops (average length 8-9 residues[81]), the CDR-H3 of 5F2 Fab includes 13 amino acid residues. However, the length of the loop is not uncommon for human antibodies.[81] The amino acid composition of CDR-H3 with the high abundance of aromatic residues corresponds well with the typical CDR-H3 loops. In the tip of the loop, two adjacent hydrophobic residues Leu102H and Trp103H create a hydrophobic patch on the antibody surface.

4.3.1 THE TESTOSTERONE BINDING SITE

The solved structure shows that testosterone is almost completely buried in the deep binding pocket of 5F2 Fab. Upon binding, 88% (402 Å^2) of the solvent accessible surface of testosterone (457 Å^2) buries. The interface area of the antibody is 233 Å^2, where the heavy chain contribution (84% of the buried surface) is substantially higher than the light chain contribution (16% of the buried surface). The D-ring of the testosterone is oriented toward the bottom of the binding pocket, which is analogous with the conjugation position to the carrier protein. The interactions between the antibody and the hapten are mainly hydrophobic and aromatic amino acid residues occupy a central role when binding the testosterone (Figure 11). The antibody binds the hapten principally through CDR-L3, CDR-H2 and CDR-H3 loops. The light chain CDR-loops L1 and L2 and the heavy chain CDR-H1 are not in contact with the hapten. These CDRs are not in the centre of the binding site and are usually in contact only with large antigens.[79]

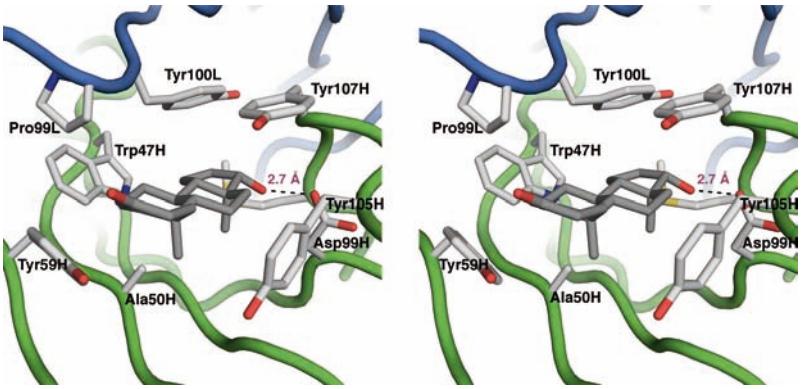

Figure 11. A stereo view of the testosterone binding site of the 5F2 Fab. The single hydrogen bond between the 5F2 Fab and the testosterone is shown as a broken black line.

In total, 8 residues from the heavy chain and 2 residues from the light chain of 5F2 Fab interact with testosterone. The α-side of the steroid skeleton packs against two aromatic residues (Tyr100L and Tyr107H) and the β-side with two methyl groups is directed against the heavy chain of the antibody. Trp47H and Tyr105 are at opposite sides of the pocket, binding the testosterone in a perpendicular alignment with respect to the side-chains of the amino acid residues. Tyr59H on the solvent exposed surface of the antibody and the other light chain residue Pro99L interact with the A-ring and the B-ring of the testosterone. Three residues from CDR-H3 loop (Asp99H, Gly108H and Met109H) form the bottom of the binding pocket. The single hydrogen bond is formed between the 17-hydroxyl group of the testosterone and the side-chain of Asp99H. Buried water molecules were not detected inside the binding pocket of 5F2 Fab.

4.3.2 STEROID BINDING ANTIBODIES

Steroids are small hydrophobic molecules, which are structurally closely related to each other. Since they are important compounds for diagnostics and therapeutic purposes, several antibodies have been generated against steroid molecules. The crystal structures of antibodies that specifically bind the major female sex hormones estrogen[82,83] and progesterone[84], male sex hormone testosterone[37,85], digoxin[86,87] and steroid glucuronides[88], have been determined by X-ray crystallography. The orientation of the steroid molecule in the binding site, the number of hydrogen bonds between the antibody and the hapten and the heavy and light chain contribution to hapten binding vary among the antibody-steroid complexes. Common to all these structures is the hydrophobic binding site with its high abundance of aromatic amino acid residues and high shape complementarity between the antibody and the hapten. Previously, the crystal structure of an *in vitro* affinity and specificity matured Fab fragment (Fab 77) from a mouse monoclonal antibody[89] was determined in free form and in complex with testosterone.[37] The comparison of free and hapten-bound structures showed that Fab 77 undergoes conformational changes when it binds testosterone. Since the attempts to crystallize 5F2 Fab without the hapten were not successful, a free form structure is not available for the detection of possible hapten-induced conformational changes in 5F2 Fab.

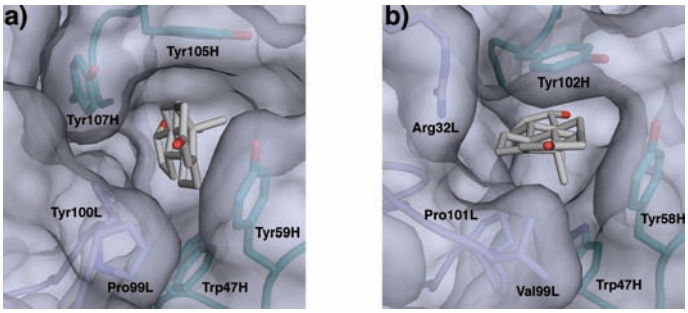

Figure 12. Binding of testosterone to 5F2 Fab (a) and to 77 Fab (b).

The sequence identity between 5F2 Fab and 77 Fab is lower for the light chain (44%) than for the heavy chain (71%). In both the 5F2 Fab and 77 Fab structures, testosterone is bound to the deep and hydrophobic pocket lined by the side-chains of aromatic amino acid residues. In the Fab 77-testosterone complex, the buried surface area of the hapten (92%) and the interface area of the antibody (234 Å^2) are similar to the 5F2 Fab complex structure. The light chain of Fab 77 contributes more to hapten binding (38% of the total buried surface area) than the light chain of 5F2 Fab. Fab 77 binds testosterone in a sandwich between the side-chains of Trp47H and Tyr102H. The corresponding aromatic amino acid residues are found in the binding site of 5F2, but the relative orientation of testosterone is different between these two Fab fragments (Figure 12). Compared with the Fab 77-testosterone structure, the hapten is turned almost 90 degrees in the 5F2 Fab-testosterone complex. The different orientation of the

bound hapten molecule seems to result from Tyr100L and Tyr107H, which occur in the binding site of 5F2 Fab and interact with the α-side of the testosterone. Besides the direct hydrogen bond between the 17-hydroxyl group of the testosterone, a buried water molecule in the binding site of Fab 77 makes possible the indirect hydrogen bonding between the D-ring hydroxyl of testosterone and the main-chain of Ala33H and the side-chain of Ser35H. Thus, the closer fit between the testosterone and antibody, as well as the hydrogen bond interactions, are likely responsible for the nanomolar binding affinity of Fab 77 ($K_d = 3 \times 10^{-10}$ M), whereas the binding affinity of 5F2 Fab to testosterone is ~ 10^{-7} M.

4.4 THE ANTI-TETRAHYDROCANNABINOL FAB FRAGMENT T3^V

The crystal structures of a T3 Fab in free form and in complex with tetrahydrocannabinol were solved at 1.9 Å and 2.0 Å resolution, respectively. The asymmetric unit of both forms contained one T3 Fab fragment. The electron density maps of the structures were of good quality and easy to interpret, with the exception of the flexible loops in the heavy chain regions of Ala134H-Met139H and Pro188H-Val197H. CDR-loops were well ordered in both the free and the complex structures. Three CDR-loops of the light chain and the heavy chain CDR-loops H1 and H2 could be classified into the known canonical structure classes.

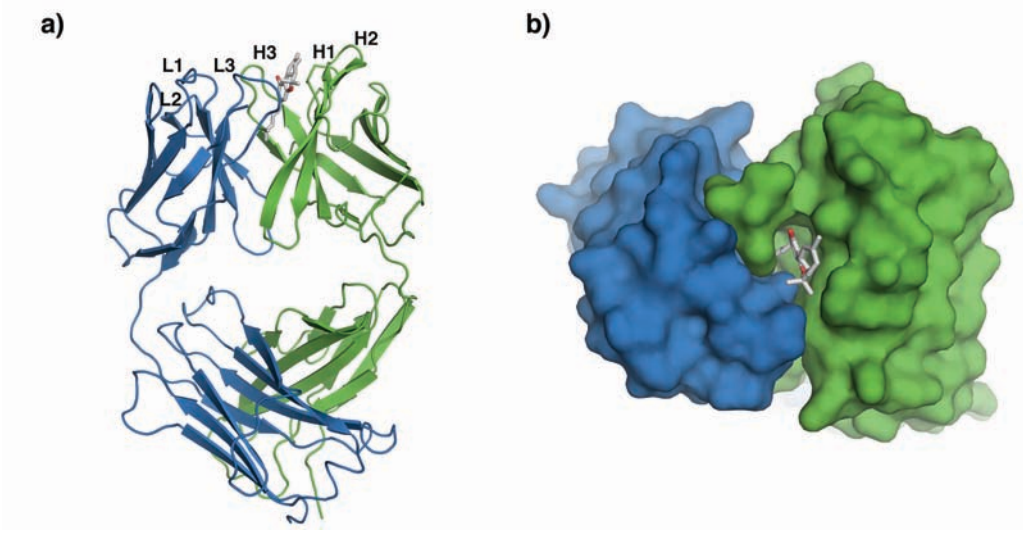

Figure 13. The overall structure of the T3 Fab-tetrahydrocannabinol complex. The T3 Fab fragment is shown as a cartoon model (a) and a surface model (b), THC is in gray.

Due to the length and the amino acid compositions of the CDR-loops, T3 Fab does not represent a typical hapten binding antibody. All six CDR-loops are relatively short, and thereby the surface of the antigen binding site is rather planar (Figure 13a). The amino

acid sequences within CDR-regions, especially within the H3-loop, are also fairly unusual. A typical CDR-H3 region is often rich in tyrosine, glycine and serine, rather than in hydrophobic residues with small side-chains, such as isoleucine and valine.[90] The CDR-H3 of T3 Fab does not contain any aromatic residues, but the loop is mainly constructed from aliphatic amino acid residues.

4.4.1 THE TETRAHYDROCANNABINOL BINDING SITE

The T3 Fab binds the tetrahydrocannabinol into a narrow hydrophobic cavity, which is located between the variable domains of the heavy chain and the light chain. In the complex structure, 469 Å^2 (84%) of the total solvent accessible surface of THC (557 Å^2) is buried. The *n*-pentyl side-chain of THC, which is attached to the C3 carbon of the phenolic ring, buries deep into the interface area of the variable domains, whereas the C10 monoterpene part of the hapten is partially exposed to the solvent (Figure 13a, 13b). The long hydrocarbon tail of the hapten molecule is able to reach four framework residues, which are highly conserved in the antibody structure.[91] This is possible because the T3 Fab has a glycine near the C-terminus of the CDR-H3 loop. The position is often occupied by a bulky amino acid residue, which blocks the entry to the interior of an antibody. 249 Å^2 of the solvent accessible surface of the antibody is buried in an antibody-antigen interface, and the heavy chain contribution on the buried surface area is 78%. All CDR-loops of the heavy chain and the CDR-3 loop of the light chain, together with five amino acids from the framework region interact with the hapten.

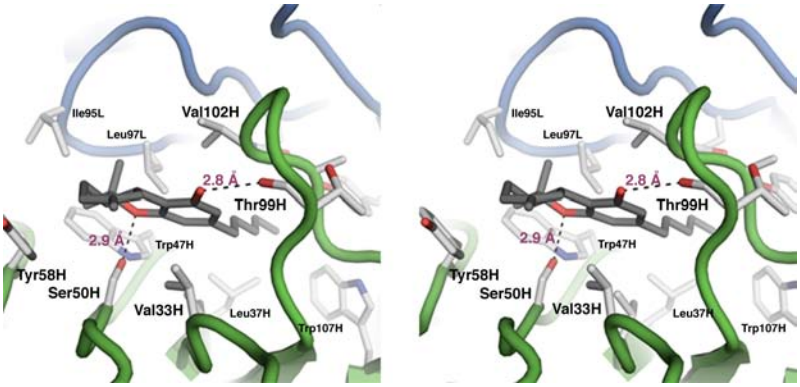

Figure 14. The binding of tetrahydrocannabinol to T3 Fab, shown in stereo. Hydrogen bonds are shown as broken black lines.

The binding site of the T3 Fab is mainly formed from aliphatic amino acid residues (Figure 14). The T3 Fab binds the *n*-pentyl side-chain of THC mainly through residues from CDR-H1 (Val35H) and CDR-H3 (Gly98H, Val102H, Ala103H, Gly104H) regions. Val33H and Val35H from CDR-H1, Gly98H and Val102H from CDR-H3,

together with Leu97L from CDR-L3 surround the phenolic ring of THC and create a hydrophobic batch around the aromatic ring. The rest of the binding interactions are directed towards the monoterpene moiety of the THC. The aromatic amino acid residues, Trp47H from the framework region and Tyr58H from CDR-H2, form an edge for the binding site. Ile95L is located near the solvent exposed surface of the antibody and makes contacts with the methyl groups of THC. The two polar groups of hapten are hydrogen-bonded with an antibody. The ether oxygen of the heterocyclic ring of THC forms a hydrogen bond with the Ser50H from CDR-H2. The second hydrogen bond is formed between the aromatic hydroxyl group of THC and the main-chain oxygen of Thr99H. Besides the four water molecules, which are displaced by THC in the complex structure, the electron density maps did not reveal other ordered water molecules or unexplained density inside the deep binding pocket of the free T3 Fab structure.

4.4.2 HAPTEN-INDUCED CONFORMATIONAL CHANGES

The comparison between the free form and complex structure shows that the T3 Fab does not undergo any large conformational rearrangements upon hapten binding. The calculated elbow angles are 156° and 157° for the free and the hapten-bound structures, respectively. The rmsd values between the Cα atoms of the free and the complex structures are 0.27 Å for the variable domain and 0.42 Å for the constant domain, which also indicate only subtle differences between the structures. Although the main-chain is highly similar in both structures, some minor changes were observed in the side-chain conformations of amino acid residues. Small adjustments of the side-chain conformations of Ile95L, Leu97L, and Val33H slightly expanded the binding cavity and improved the fit between the THC and T3 Fab (Figure 15a, 15b).

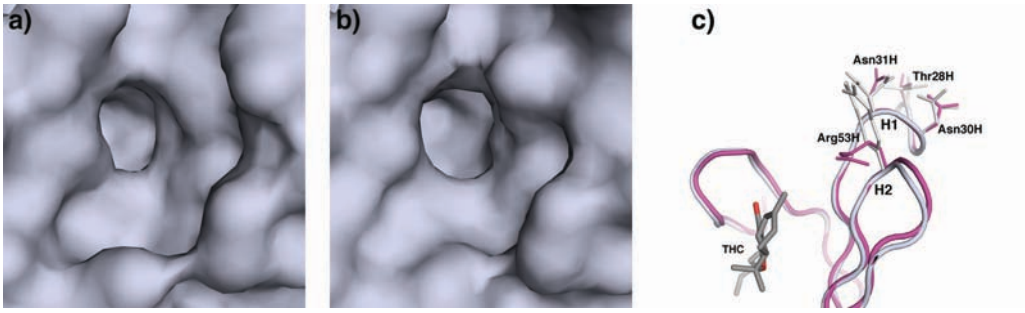

Figure 15. The hapten-induced conformational changes. Binding site of T3 Fab in free form (a) and in complex structure (b) shown as surface models. c) Conformations of four amino acids near the binding site of T3 Fab. The free form structure is shown in magenta and the complex structure is in gray.

Four residues (Thr28H, Asn30H, Asn31H, Arg53H) on the solvent exposed surface of the T3 Fab appear to have additional conformations in the complex structure. Two

favorable side-chain conformations were refined for each of these amino acids. One of these two conformations was observed in the free T3 Fab structure, with the exception of Arg53H, which occupies a distinct side-chain conformation (Figure 15c). These amino acids are not in contact with the bound hapten molecule, but they may influence the recognition mechanism of the secondary antibody.

4.4.3 THE BINDING OF A PSYCHOACTIVE CANNABINOID TO AN ANTIBODY

Tetrahydrocannabinol is a hydrophobic terpenophenolic compound, whose crystal structure has not been previously characterized by X-ray crystallography. The conformation of the Δ^9-THC skeleton has been established by solving the crystal structures of the psychotropically inactive Δ^9-tetrahydrocannabinol acid B[92] and the moderately active 8β-hydroxy-Δ^9-tetrahydrocannabinol.[93] The stereochemistry of the THC in the binding site of the T3 Fab presents the natural active *trans* (6aR, 10aR) isomer conformation. As with the two previously determined cannabinoids, THC occurs in a bent conformation in the complex structure.

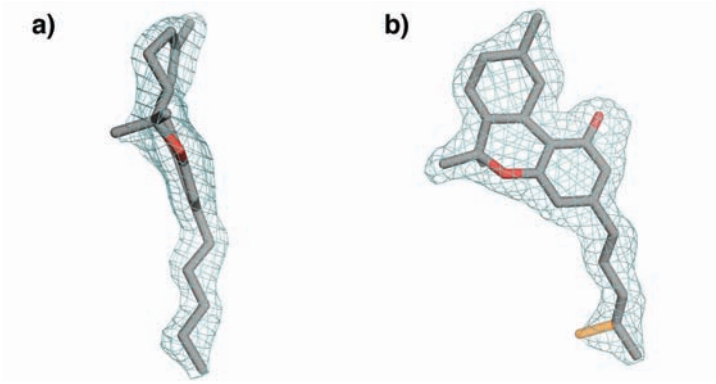

Figure 16. a, b) The Fo-Fc omit map for the bound THC molecule contoured at 2.5 σ. b) The *n*-pentyl side-chain of THC adopts both the *anti* and the *gauche* conformations in the binding site of T3 Fab. The *gauche* conformation is shown in orange.

Both the cyclohexene ring and the phenol ring of THC occur in a half-chair conformation. The cyclohexene ring and the *n*-pentyl side-chain are located on the opposite sides of the planar phenol group (Figure 16a). The binding site of the T3 Fab is narrow, but the terminal methyl group of the side-chain of THC is still capable of rotating around the single carbon-carbon bond. Based on the electron density maps, the *n*-pentyl chain was found to occur in both the fully extended all-*anti* conformation and the *gauche*-conformation with respect to the C4´-C5´ bond (Figure 16b).

5 CONCLUSIONS

In order to understand the molecular basis for the antibody specificity and binding affinity, the crystal structures of three different antibody-antigen complexes were determined by X-ray crystallography. The crystal structures of the IgE antibody-allergen complex D1/BLG, the anti-testosterone Fab fragment 5F2 and the anti-tetrahydrocannabinol Fab fragment T3 allowed the detailed identification of antibody-antigen interactions and increased the knowledge of the recognition mechanisms of the antibodies. The solved structures are also expected to facilitate the design of specific modifications that could enhance the binding properties of the antibodies.

The three-dimensional structure of the complex between the IgE Fab fragment D1 and the dimeric bovine beta-lactoglobulin allergen was solved at 2.8 Å resolution. This was the first structure of the IgE antibody-allergen immunocomplex and revealed the complete IgE epitope of an allergen, which was found to differ from common IgG epitopes of protein antigens. The findings that IgE antibodies seem to prefer different binding sites than the common IgG antibodies and that the protein oligomerization may increase its allergenicity could lead to novel approaches to the treatment of allergy.

The combination of polystyrene nanospheres and the streak-seeding method was found to be an efficient technique for producing well-ordered protein crystals. The 5F2 Fab-testosterone crystals that were obtained using this novel optimization strategy diffracted the synchrotron radiation up to 1.5 Å resolution. However, the twinning that occurred in the 5F2 Fab crystal complicated the structure determination. The twinning was not detectable from diffraction images and was not suspected until the refinement of the structure proved to be difficult. Pseudomerohedral twinning, where a triclinic crystal mimics a monoclinic one, has not been previously reported for protein crystals, so the type of twinning in the 5F2 Fab crystal was therefore difficult to identify. The solved structure showed that the binding site of the 5F2 Fab to testosterone is a deep hydrophobic pocket, which is located between the variable domains of the antibody. The high contribution of the aromatic amino acid residues towards hapten binding and the good shape complementarity between the antibody and the hapten was comparable with previously determined antibody-steroid structures.

The crystal structure of the anti-tetrahydrocannabinol binding Fab fragment T3 was solved in free form at 1.9 Å resolution and in complex with THC at 2.0 Å resolution. The combination of the nanospheres and the seeding substantially enhanced the quality of the T3 Fab-THC crystals. The binding mechanism of a psychoactive cannabinoid to protein had not been determined by X-ray crystallography before this study. The T3 Fab was found to bind the hapten into a narrow and deep pocket. The analysis of the binding interactions proved that the T3 Fab binds the hydrophobic cannabinoid molecule mainly through aliphatic amino acid residues and that the highly conserved amino acids from the framework region of the T3 Fab also interact with the hapten. The comparison between the free and THC-bound structures showed that large conformational changes do not occur in the T3 Fab when it binds hapten.

ACKNOWLEDGEMENTS

This work was carried out at the Department of Chemistry, University of Eastern Finland, Joensuu, between 2004-2010. I would like to gratefully acknowledge The National Graduate School in Informational and Structural Biology and the Sigrid Jusélius Foundation for their financial support towards this study.

I am most indebted to my supervisor, Prof. Juha Rouvinen, for introducing me to the field of protein crystallography, and for his support and invaluable advice. The members of the "Origin of Allergy" team, Prof. Tari Haahtela and Docent Soili Mäkinen-Kiljunen from Helsinki University Central Hospital, Prof. Hans Söderlund, Prof. Kristiina Takkinen, Dr. Marja-Leena Laukkanen and Sirpa Jylhä from the VTT Technical Research Centre of Finland, are also sincerely acknowledged for their fruitful collaboration and inspiring discussions. I am grateful to all people from VTT that enabled this study by providing protein material and for sharing their knowledge of antibodies with us. I would especially like to thank Prof. Kristiina Takkinen, for her kind assistance during these years.

I am deeply grateful to the present and former members of the protein crystallography group. I want to thank you not only for the great help and encouragement you have provided me with but also for your excellent company during these years. In particular, I would like to thank Dr. Jarkko Valjakka for helping me with the antibody structures at the beginning of this study and Dr. Nina Hakulinen for her skilful guidance and her positive attitude that made the days brighter. I would like to thank my office colleagues, Dr. Tarja Parkkinen and Juha Kallio, for their patience, and Dr. Johanna Kallio and Mirko Maksimainen for their company during work trips. I also am grateful to Prof. Janne Jänis, for determining the mass spectra and cheering me up whenever I needed it. I also wish to thank Dr. Elina Kalenius for being a friend both at and outside of work. The entire staff of the Department of Chemistry should also be recognized for helping to create a pleasant working environment, thank you.

Finally, I warmly thank my brothers and their families, and my friends, for their invaluable support. I would also like to remember my late father who encouraged me to study, as I owe him and my mother special thanks for their infinite support and care.

REFERENCES

1. Schiffer, M., Girling, R. L., Ely, K. R. and Edmundson, A. B. *Biochemistry* **12** (1973) 4620.

2. Poljak, R. J., Amzel, L. M., Avey, H. P., Chen, B. L., Phizackerley, R. P. and Saul, F. *Proc. Natl. Acad. Sci.* **70** (1973) 3305.

3. Harris, L. J., Larson, S. B., Hasel, K. W. and McPherson, A. *Biochemistry* **36** (1997) 1581.

4. Galli, S. J., Tsai, M. and Piliponsky, A. M. *Nature* **454** (2008) 445.

5. Aalberse, R. C. *J. Allergy Clin. Immunol.* **106** (2000) 228.

6. Jenkins, J. A., Griffith-Jones, S., Shewry, P.R., Breiteneder, H. and Mills, E. N. C. *J. Allergy Clin. Immunol.* **115** (2005) 163.

7. Radauer, C., Bublin, M., Wagner, S., Mari, A. and Breiteneder, H. *J. Allergy Clin. Immunol.* **121** (2008) 847.

8. Hantusch, B., Schöll, I., Harwanegg, C., Krieger, S., Becker, W.-M., Spitzauer, S., Boltz-Nitulescu, G. and Jensen-Jarolim, E. *Immunol. Lett.* **97** (2005) 81.

9. Saarelainen, S., Zeiler, T., Rautiainen, J., Närvänen, A., Rytkönen-Nissinen, M., Mäntyjärvi, R., Vilja, P. and Virtanen, T. *Int. Immunol.* **14** (2002) 401.

10. Larché, M., Akdis, C. A. and Valenta, R. *Nat. Rev. Immunol.* **6** (2006) 761.

11. Laver, W. G., Air, G. M., Webster, R. G. and Smith-Gill, S. J. *Cell* **61** (1990) 553.

12. Winter, G., Griffiths, A. D., Hawkins, R. E. and Hoogenboom, H. R. *Annu. Rev. Immunol.* **12** (1994) 433.

13. Vaughan, T. J., Williams, A. J., Pritchard, K., Osbourn, J. K., Pope, A. R., Earnshaw, J. C., McCafferty, J., Hodits, R. A., Wilton, J. and Johnson, K. S. *Nat. Biotechnol.* **14** (1996) 309.

14. Hoogenboom, H. R., de Bruine, A. P., Hufton, S. E., Hoet, R. M., Arends, J.-W. and Roovers, R. C. *Immunotechnol.* **4** (1998) 1.

15. Hoogenboom, H. R. *Nat. Biotechnol.* **23** (2005) 1105.

16. de Haard, H., Henderikx, P. and Hoogenboom, H. R. *Adv. Drug Delivery Rev.* **31** (1998) 5.

17. Vaughan, T. J., Osbourn, J. K. and Tempest, P. R. *Nat. Biotechnol.* **16** (1998) 535.

18. Ullman, E, F., Milburn, G., Jelesko, J., Radika, K., Pirio, M., Kempe, T. and Skold, C. *Proc. Natl. Acad. Sci.* **90** (1993) 1184.

19. Self, C. H., Dessi, J. L. and Winger, L. A. *Clin. Chem.* **40** (1994) 2035.

20. Towbin, H., Motz, J., Oroszlan, P. and Zingel, O. *J. Immunol. Methods* **181** (1995) 167.

21. Pulli, T., Höyhtyä, M., Söderlund, H. and Takkinen, K. *Anal. Chem.* **77** (2005) 2637.

22. Pavlou, A. K. and Belsey, M. J. *Eur. J. Pharm. Biopharm.* **59** (2005) 389.

23. Takkinen, K., Laukkanen, M.-L., Sizmann, D., Alfthan, K., Immonen, T., Vanne, L., Kaartinen, M., Knowles, J. K. and Teeri, T. T. *Protein Eng*. **4** (1991) 837.

24. Jylhä, S., Mäkinen-Kiljunen, S., Haahtela, T., Söderlund, H., Takkinen, K. and Laukkanen, M.-L. *J. Immunol. Methods* **350** (2009) 63.

25. Kabsch, W. *J. Appl. Cryst*. **26** (1993) 795.

26. Jones, T. A., Zou, J. - Y., Cowan, S. W. and Kjeldgaard, M. *Acta Cryst*. A**47** (1991) 110.

27. Schuettelkopft, A. W. and van Aalten, D. M. F. *Acta Cryst*. D**60** (2004) 1355.

28. Collaborative Computational Project, Number 4. *Acta Cryst*. D**50** (1994) 760.

29. Stanfield, R. L., Zemla, A., Wilson, I. A. and Rupp, B. *J. Mol. Biol*. **357** (2006) 1566.

30. Westbrook, J., Feng, Z., Burkhardt, K. and Berman, H. M. *Meth. Enz*. **374** (2003) 370.

31. He, X. M., Ruker, F., Casale, E. and Carter, D. C. *Proc. Natl. Acad. Sci*. **89** (1992) 7154.

32. Oliveira, K. M., Valente-Mesquita, V. L., Botelho, M. M., Sawyer, L., Ferreira, S. T. and Polikarpov, I. *Eur. J. Biochem*. **268** (2001) 477.

33. Vagin, A. and Teplyakov, A. *J. Appl. Cryst*. **30** (1997) 1022.

34. Brünger, A. T., Adams, P. D., Clore, G. M., DeLano, W. L., Gros, P., Grosse-Kunstleve, R. W., Jiang, J.-S., Kuszewski, J., Nilges, M., Pannu, N. S., Read, R. J., Rice, L. M., Simonson, T. and Warren, G. L. *Acta Cryst*. D**54** (1998) 905.

35. Karpusas, M., Ferrant, J., Weinreb, P., Carmillo, A., Taylor, F. and Garber, E. *J. Mol. Biol*. **327** (2003) 1031.

36. Adams, P. D., Grosse-Kunstleve, R. W., Hung, L.-W., Ioerger, T. R., McCoy, A. J., Moriarty, N. W., Read, R. J., Sacchettini, J., C., Sauter, N. K. and Terwilliger, T. C. *Acta Cryst*. D**58** (2002) 1948.

37. Valjakka, J., Hemminki, A., Niemi, S., Söderlund, H., Takkinen, K. and Rouvinen, J. *J. Biol. Chem*. **277** (2002) 44021.

38. Oda, M., Ito, N., Tsumuraya, T., Suzuki, K., Sakakura, M. and Fujii, I. *J. Mol. Biol*. **369** (2007) 198.

39. McCoy, A. J., Grosse-Kuntsleve, R. W., Adams, P. D., Winn, M. D., Storoni, L. C. and Read, R. J. *J. Appl. Cryst*. **40** (2007) 658.

40. Parson, S. *Acta Cryst*. D**59** (2003) 1995.

41. Dauter, Z. *Acta Cryst*. D**59** (2003) 2004.

42. Mueller, U., Muller, Y. A., Herbst-Irmer, R., Sprinzl, M. and Heinemann, U. *Acta Cryst*. D**55** (1999) 1405.

43. Brownlow, S., Cabral, J. H. M., Cooper, R., Flower, D. R., Yewdall, S. J., Polikarpov, I., North, A. C. T. and Sawyer, L. *Structure* **5** (1997) 481.

44. Wu, S. -Y., Pérez, M. D., Puyol, P. and Sawyer, L. *J. Biol. Chem*. **274** (1999) 170.

45. Sawyer, L. and Kontopidis, G. *Biochim. Biophys. Acta* **1482** (2000) 136.

46. Kontopidis, G., Holt, C. and Sawyer, L. *J. Mol. Biol.* **318** (2002) 1043.

47. Al-Lazikani, B., Lesk, A. M. and Chothia, C. *J. Mol. Biol.* **273** (1997) 927.

48. Morea, V., Tramontano, A., Rustici, M., Chothia, C. and Lesk, A. M. *J. Mol. Biol.* **275** (1998) 269.

49. Lo Conte, L., Chothia, C. and Janin, J. *J. Mol. Biol.* **285** (1999) 2177.

50. Davies, D. R. and Cohen, G. H. *Proc. Natl. Acad. Sci.* **93** (1996) 7.

51. Aymard, P., Durand, D. and Nicolai, T. *Int. J. Biol. Macrom.* **19** (1996) 213.

52. Verheul M., Pedersen J. S., Roefs, S. P. F. M. and de Kruif, K. G. *Biopolymers* **49** (1999) 11.

53. Kane P., Erickson, J., Fewtrell, C., Baird, B. and Holowka, D. *Mol. Immunol.* **23** (1986) 783.

54. Kane, P.M., Holowka, D. and Baird, B. *J. Cell. Biol.* **107** (1988) 969.

55. Kamata Y., Miyanomae, A., Nakayama, E., Miyanomae, T., Tajima, T., Nishimura, K., Tada, T. and Hoshi, H. *In. Arch. Allergy Immunol.* **142** (2007) 301.

56. Lascombe, M.-B., Grégoire, C., Poncet, P., Tavares, G. A., Rosinski-Chupin, I., Rabillon, J., Goubran-Botros, H., Mazie C.-J., David, B. and Alzari, P. M. *J. Biol. Chem.* **275** (2000) 21572.

57. Grönlund, H., Bergman, T., Sandström, K., Alvelius, K., Reininger, R., Verdino, P., Hauswirth, A., Liderot, K., Valent, P., Spitzauer, S., Keller, W., Valenta, R., van Hage-Hamsten, M. *J. Biol. Chem.* **278** (2003) 40144.

58. Ball, T., Edstrom, W., Mauch, L., Schmitt, J., Leistler, B., Fiebig, H., Sperr, W. R., Hauswirth, A. W., Valent, P., Kraft, D., Almo, S. C. and Valenta, R. *FEBS J.* **272** (2005) 217.

59. Verdino, P., Westritschnig, K., Valenta, R. and Keller, W. *EMBO J.* **21** (2002) 5007.

60. Shin, D. S., Compadre, C. M., Maleki, S. J., Kopper, R. A., Sampson, H., Huang, S. K., Burks, A. W. and Bannon, G. A. *J. Biol. Chem.* **273** (1998) 13753.

61. Maleki, S. J., Kopper, R. A., Shin, D. S., Park, C.-W., Compadre, C. M., Sampson, H., Burks, A. W. and Bannon, G. A. *J. Immunol.* **164** (2000) 5844.

62. Sen, M., Kopper, R., Pons, L., Abraham, E. C., Burks, A. W. and Bannon, G. A. *J. Immunol.* **169** (2002) 882.

63. Schöll, I., Kalkura, N., Shedziankova Y., Bergmann, A., Verdino, P., Knittelfelder, R., Kopp, T., Hantusch, B., Betzel, C., Dierks, K., Scheiner, O., Boltz-Nitulescu, G., Keller, W. and Jensen-Jarolim, E. *J. Immunol.* **175** (2005) 6645.

64. Mirza, O., Henriksen, A., Ipsen, H., Larsen, J. N., Wissenbach, M., Spangfort, M. D. and Gajhede, M. *J. Immunol.* **165** (2000) 331.

65. Padavattan, S., Schirmer, T., Schmidt, M., Akdis, C., Valenta, R., Mittermann, I., Soldatova, L., Slater, J., Mueller, U. and Markovic-Housley, Z. *J. Mol. Biol.* **368** (2007) 742.

66. Li, M., Gustchina, A., Alexandratos, J., Wlodaver, A., Wünschmann, S., Kepley, C. L., Chapman, M. D. and Pomés, A. *J. Biol. Chem.* **283** (2008) 22806.

67. Padavattan, S., Flicker, S., Schirmer, T., Madritsch, C., Randow, S., Reese, G., Vieth, S., Lupinek, S., Ebner, C., Valenta, R. and Markovic-Housley, Z. *J. Immunol.* **182** (2009) 2141.

68. Steinberger, P., Kraft, D. and Valenta, R. *J. Biol. Chem.* **271** (1996) 10967.

69. Flicker, S., Steinberger, P., Nordenhaugh, L., Sperr, W. R., Majlesi, Y., Valent, P., Kraft, D. and Valenta, R. *Eur. J. Immunol.* **32** (2002) 2156.

70. Laukkanen, M.-L., Mäkinen-Kiljunen, S., Isoherranen, K., Haahtela, T., Söderlund, H. and Takkinen, K. *J. Immunol. Methods* **278** (2003) 271.

71. Flicker, S., Steinberger, P., Ball, T., Krauth, M.-T., Verdino, P., Valent, P., Almo, S. and Valenta, R. *J. Allergy Clin. Immunol.* **117** (2006) 1336.

72. Jutel, M., Jaeger, L., Suck, R., Meyer, H., Math, D., Fiebig, H. and Cromwell, O. *J. Allergy Clin. Immunol.* **116** (2005) 608.

73. Reisinger, J., Horak, F., Pauli, M., van Hage, M., Cromwell, O., König, F., Valenta, R. and Niederberger, V. *J. Allergy Clin. Immunol.* **116** (2005) 347.

74. Wachholtz, P. A. and Durham, S. R. *Curr. Opin. Allergy Clin. Immunol.* **4** (2004) 313.

75. Niederberger, V. *Immunol. Letters* **122** (2009) 131.

76. Valenta, R. and Niederberger, V. *J. Allergy Clin. Immunol.* **119** (2007) 826.

77. Linhart, B. and Valenta, R. *Curr. Opin. Immunol.* **17** (2005) 646.

78. Akdis, M. A. and Akdis, C. A. *J. Allergy Clin. Immunol.* **119** (2007) 780.

79. McCallum, R. M., Martin, A. C. R. and Thornton, J. M. *J. Mol. Biol.* **262** (1996) 732.

80. Vargas-Madrazo, E., Lara-Ochoa, F. and Almagro, J. C. *J. Mol. Biol.* **254** (1995) 497.

81. Collis, A. V. J., Brouwer, A. P. and Martin, A. C. R. *J. Mol. Biol.* **325** (2003) 337.

82. Lamminmäki, U. and Kankare J. A. *J. Biol. Chem.* **276** (2001) 36687.

83. Monnet, C., Bettsworth, F., Stura, E. A., Le Du, M.-H., Ménez, R., Derrien, L., Zinn-Justin, S., Gilquin, B., Sibai, G., Battail-Poirot, N., Jolivet, M., Ménez, A., Arnaud, M., Ducancel, F. and Charbonnier, J. B. *J. Mol. Biol.* **315** (2002) 699.

84. Arevalo, J. H., Hassig, C. A., Stura, E. A., Sims, M. J., Taussig, M. J. and Wilson, I. A. *J. Mol. Biol.* **241** (1994) 663.

85. Valjakka, J., Takkinen, K., Teerinen, T., Söderlund, H. and Rouvinen, J. *J. Biol. Chem.* **277** (2002) 4183.

86. Jeffrey, P. D., Strong, R. K., Sieker, L. C., Chang, C. Y. Y., Campbell, R. L., Petsko, G. A., Haber, E., Margolies, M. N. and Sheriff, S. *Proc. Natl. Acad. Sci.* **90** (1993) 10310.

87. Jeffrey, P. D., Schildbach, J. F., Chang, C. Y. Y., Kussie, P. H., Margolies, M. N. and Sheriff, S. *J. Mol. Biol.* **248** (1995) 344.

88. Trinh, C. H., Hemmington, S. D., Verhoeyen, M. E. and Phillips, S. E. V. *Structure* **5** (1997) 937.

89. Hemminki, A., Niemi, S., Hoffrén, A.-M., Hakalahti, L., Söderlund, H. and Takkinen, K. *Protein Eng*. **11** (1998) 311.

90. Zemlin, M., Klinger, M., Link, J., Zemlin, C., Bauer, K., Engler, J. A., Schroeder, H. W. Jr. and Kirkham, P. M. *J. Mol. Biol*. **334** (2003) 733.

91. Chothia, C., Gelfand, I. and Kister, A. *J. Mol. Biol*. **278** (1998) 457.

92. Rosenqvist, E. and Ottersen, T. *Acta Chem. Scand. B* **29** (1975) 379.

93. Ottersen, T. and Rosenqvist, E. Acta *Chem. Scan. B* **31** (1977) 749.

76/2005 MORENO M. Andreina: Ruthenium and iridium carbonyls. Catalytic activity and formation of ruthenium complexes containing aromatic nitrogen donor and phosphane ligands

77/2006 VENTOLA Elina: Host-guest chemistry of resorcarene derivatives studied by ESI-FTICR mass spectrometry

78/2006 HAKANPÄÄ Johanna: Structural studies of *Trichoderma reesei* hydrophobins HFBI and HFBII – the molecular basis for function of fungal amphiphiles

79/2006 ORESMAA Larisa: Synthesis, characterization and nitric oxide donation of imidazole nitrolic acids and amidoximes and their esters

80/2006 KOPONEN Markus: Noble metal promoted perovskites: reactivity and catalytic activity

81/2006 NEITOLA Raisa: *Ab initio* studies on the atomic-scale origin of friction between interacting surfaces: diamond, fluorinated diamond, graphite, and hydrocarbons

82/2006 HILTUNEN Eveliina: Phenolic extractives and discolouration of dried silver and white birch (*Betula pendula* and *Betula pubescens*) wood

83/2006 HOLOPAINEN Timo: Studies on phenol-formaldehyde resol resins for adhesives and overlays

84/2006 TURUNEN Jani: The role of mesoporous silica and alumina as metallocene catalyst supports in the formation of polyethylene nanofibers

85/2007 PUUKILAINEN Esa: Chemically modified and surface structured hydrophobic polyolefins

86/2007 KARTTUNEN Antti: Structural principles of group 14 icosahedral hydrides and elemental nanostructures of phosphorus and arsenic

87/2007 KOPONEN Hanna-Kaisa: Soiling and wetting of polymers: smooth and structured poly(vinyl chloride) and cycloolefin copolymer surfaces

88/2007 PAUNIKALLIO Teemu: Tailoring the adhesion in viscose fiber reinforced polypropylene and polyamide composites

89/2007 JAKONEN Minna: Surface-assisted synthesis of ruthenium, rhodium, and osmium carbonyl complexes, and effect of ligands on their behavior

90/2007 KOSKILINNA Jussi: Quantum chemical studies on atomic-scale tribology of diamond and boron nitride

91/2007 MARJASVAARA Asse: Mass spectrometric characterization of laccases: their catalyzing properties and molecular structure

92/2008 HIRVI Janne: Wetting of smooth and nanostructured polyethylene and polyvinylchloride surfaces studied by molecular dynamics simulations

93/2008 MIIKKULAINEN Ville: Molybdenum nitride thin films on micro- and nanopatterned substrates: atomic layer deposition and applications

94/2008 MONNI Janne: Controlled synthesis, curing, and modification of phenol-formaldehyde resol resins

95/2008 PARKKINEN Tarja: Structural studies on proteins with industrial potential: ENA11His Fab fragment, *Streptomyces rubiginosus* xylose isomerase, *Trichoderma reesei* xylanase IV and *Melanocarpus albomyces* cellobiohydrolase

96/2008 KARTTUNEN Virve: The influence of ligand structure of hafnocene catalysts on ethene polymerization studied by quantum chemical methods

97/2008 TANSKANEN Jukka: One- and two-dimensional nanostructures of group 14 elemental hydrides and group 13-15 binary hydrides

98/2009 JOKINIEMI Jonna: Structural studies on metal complexes of mixed amide esters and phenyl and monoalkyl ester derivatives of dichloromethylene biphosphonic acid

99/2009 KALIMA Valtteri: Controlled replication of patterned polymer and nanocomposite surfaces for micro-optical applications

100/2009 HYYRYLÄINEN Anna: Differeniation of diastereomeric and enantiomeric β-amino acids by mass spectrometry

101/2010 KUNNAS-HILTUNEN Susan: Synthesis, X-ray diffraction study and characterisations of metal complexes of clodronic acid and its symmetrical dianhydride derivatives